

Early Cretaceous dendritic shrub-like fabric in karstified peritidal carbonates from southern Italy

Sabrina Amodio ^{a,*}, Filippo Barattolo ^b, Robert Riding ^c

^a DiST, Dipartimento di Scienze e Tecnologie, Università degli Studi di Napoli "Parthenope", Centro Direzionale Isola C4, 80143 Napoli, Italy

^b DiSTAR, Dipartimento di Scienze della Terra, dell'Ambiente e delle Risorse, Università degli Studi di Napoli Federico II, Largo San Marcellino, 10, 80138 Napoli, Italy

^c Department of Earth and Planetary Sciences, University of Tennessee, Knoxville, TN 37996–1526, USA



ARTICLE INFO

Article history:

Received 6 April 2018

Received in revised form 1 June 2018

Accepted 6 June 2018

Available online 09 June 2018

Editor: Dr. B. Jones

Keywords:

Cryptic carbonate shrub-like fabric

Microkarst

Valanginian

Southern Apennines

Italy

ABSTRACT

Lower Cretaceous (Valanginian) dendritic microfabrics occur in karstic cavities within fine-grained shallow-marine platform carbonates at San Lorenzello, southern Italy. They form dense micritic masses and clusters, generally oriented perpendicularly to cavity surfaces, surrounded by layered sparry cement. Individual dendrites, typically sub-millimetric in size, have highly irregular margins and form distinctive shrub-like masses ranging from compact and squat, to elongate and highly branched. The centimetric and irregularly elongate cavities appear to have formed through subaerial exposure, and are almost entirely filled by the micritic dendrites and associated sparry crusts. In size, shape and micritic composition, the dendrites broadly resemble a variety of similar fabrics, including hot spring travertine shrubs and calcified microfossils such as Cambrian *Angusticellularia*, which has analogs in present-day lacustrine calcified cyanobacteria. However, the San Lorenzello dendrites differ in occupying small cavities. This cryptic microkarstic dripstone setting, together with the often regular spacing and appearance of these dendritic fabrics, may be more consistent with an abiotic origin. These comparisons underscore the challenge of interpreting microdendritic carbonate fabrics in general.

© 2018 Elsevier B.V. All rights reserved.

1. Introduction

A wide variety of small calcified dendritic structures occur in the geological record of marine and continental carbonates. Some are organic in origin, and include calcimicrobes, commonly regarded as algae or cyanobacteria, that are abundant in Cambrian and Late Devonian reefs (Pratt, 1984; Riding and Voronova, 1985; Riding, 1991a). Others are almost certainly abiotic, such as crystal shrubs in hot spring travertine deposits (Pentecost, 1990; Chafetz and Guidry, 1999; Gandin and Capezzuoli, 2014). But there are many examples whose origins are less clear. Carbonate shrubs have been described from the lower member of the Noonday Dolomite, Neoproterozoic in age (Death Valley region, USA, Fraiser and Corsetti, 2003) as well as in ambient water Eocene lacustrine carbonates of the Green River formation (Wyoming, USA; Seard et al., 2013). At the present day, carbonate shrubs occur in hot water travertine deposits (e.g. Chafetz and Guidry, 1999; Della Porta, 2015; Erthal et al., 2017) and in ambient temperature travertine systems (e.g. Anzalone et al., 2007; Golubić et al., 2008; Seard et al., 2013). The difficulty of interpreting shrub-like structures with irregular dendritic arrangement and crystalline or micritic fabrics arises from their morphological simplicity and wide distribution. Depositional environment would seem to be a useful guide to whether these fabrics are biotic or abiotic. For example,

dendritic fabrics in marine reefs and freshwater creeks could be more likely to be organic than similar fabrics in hot spring deposits. However, microbial carbonates can form in all these environments, and some hot spring travertine shrubs have long been interpreted as bacterial in origin (Chafetz and Folk, 1984; Koban and Schweigert, 1993; Cook and Chafetz, 2017). As a result, there are numerous examples of carbonate dendrites whose origins remain uncertain (Jones and Renaut, 1995, 2010; Erthal et al., 2017) and which, in a further complication, may have been produced by a combination of biotic and abiotic processes (Guo and Riding, 1994; Jones and Kahle, 1995). Most ancient examples of carbonate shrub fabrics have been described from Paleozoic marine environments, whereas most present-day examples occur in hot spring travertines. Here we describe Early Cretaceous dendritic fabrics that occur in peritidal limestones that appear to have been influenced by karstification during subaerial exposure. These examples can be compared in shape and size to a wide variety of fossil and extant shrub fabrics but are unusual due to their age, cryptic dripstone environmental setting, and complex diagenetic history.

2. Geological and stratigraphic settings

The dendritic fabrics described here occur in Valanginian limestones at San Lorenzello, in a well-exposed section of the thick Early Cretaceous shallow water carbonate succession that is widespread in the southern Apennines, Italy. The section is located on the south-eastern slope of the

* Corresponding author.

E-mail address: sabrina.amodio@uniparthenope.it (S. Amodio).

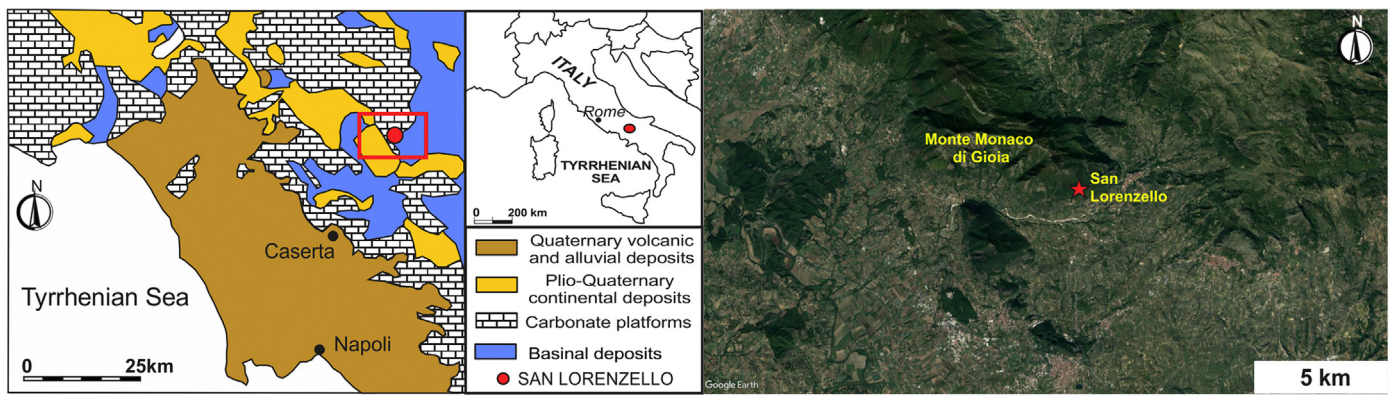


Fig. 1. Geological setting and location of the San Lorenzello section. (For interpretation of the references to color in this figure, see the web version of this article.)

Monte Monaco di Gioia (Matese Mountains, Campania), 70 km north of Naples (Fig. 1, Amodio, 2006; Amodio et al., 2008a, b), along the road from San Lorenzello to the viewpoint of Colle la Sella-La Pizzuta. Monte Monaco di Gioia is part of the Southern Apennine N-E verging fold and thrust belt, produced by Apulian–Ionian composite plate migration (Malinverno and Ryan, 1986; Patacca and Scandone, 2007; D’Argenio et al., 2011) during Africa–Europe collision. This deformation history started with late Triassic–Liasic rifting, which fragmented a tropical intracratonic carbonate platform into a number of carbonate platforms and basins (Mostardini and Merlini, 1986; Patacca and Scandone, 2007). These paleogeographic domains were part of Adria (also called Apulia) on the continental margin to the south of the Alpine Tethys Ocean (Fig. 1). During the Late Cretaceous, they were progressively incorporated into the Alpine–Apennine–Dinaric orogenic system by collision of the Euro-Asiatic and Afro-Adriatic continental margins (Malinverno and Ryan, 1986; Shiner et al., 2004; Vitale and Ciarcia, 2013). Current paleogeographic reconstructions infer two large carbonate platforms, the Apennine platform to the west and the Apulia platform to the east, separated by the Lagonegro Basin (Mostardini and Merlini, 1986; Vitale and Ciarcia, 2013). In this context, the San Lorenzello section is part of the Apennine platform.

The San Lorenzello section is about 86 m thick and Late Valanginian–Early Hauterivian in age. In the last two decades, detailed studies of the biostratigraphy, sedimentology, cyclostratigraphy and sequence-stratigraphy (D’Argenio et al., 1997; Ferreri et al., 2004; Amodio, 2006) have been carried out (Fig. 2). The section consists of well-bedded gray limestones and whitish to gray dolomitic limestones (wackestones, packstones) with benthic foraminifers, green algae and molluscs (subtidal deposits). Mudstone and loferitic mudstone-wackestone (peritidal deposits) horizons are subordinate. High-energy deposits of intraclasts and bioclasts with erosional bases locally form episodic intercalations (tempestites). A hierarchy of shallowing-upward cycles (elementary cycles, bundles, superbundles), which can be linked to orbital oscillations, shows a good fit with the Valanginian–Hauterivian time scale (Ferreri et al., 2004). Bulk carbonate carbon-isotope values of a high-resolution curve also show a similar response to original climate-ocean forcing (Amodio et al., 2008a, b). C-isotope correlation of these data with coeval curves from the hemipelagic La Charce (Vocontian Basin, France) and pelagic Capriolo (southern Alps, northern Italy) sections assists recognition of the Valanginian–Hauterivian boundary at San Lorenzello, about 50 m from the base of the section (Amodio et al., 2008a, b).

3. Methods

Re-sampling of the San Lorenzello section for micropaleontological and biostratigraphical analyses revealed a 30 cm-thick horizon containing dendritic fabric, 37 m above the base of the section in the uppermost Valanginian (see red star in Fig. 2). Detailed stratigraphic description and facies analysis in the field, using a 10× hand lens, was integrated

with examination of 15 thin sections and about 10 polished slabs, using standard petrographic techniques to recognize textures, grains (skeletal, non-skeletal), and sedimentary and diagenetic structures. Additional thin-section studies were made to elucidate cement types and their sequence of development to characterize the cavity-fillings deposits in which the dendrites occur.

4. Carbonate dendritic facies and its environmental interpretation

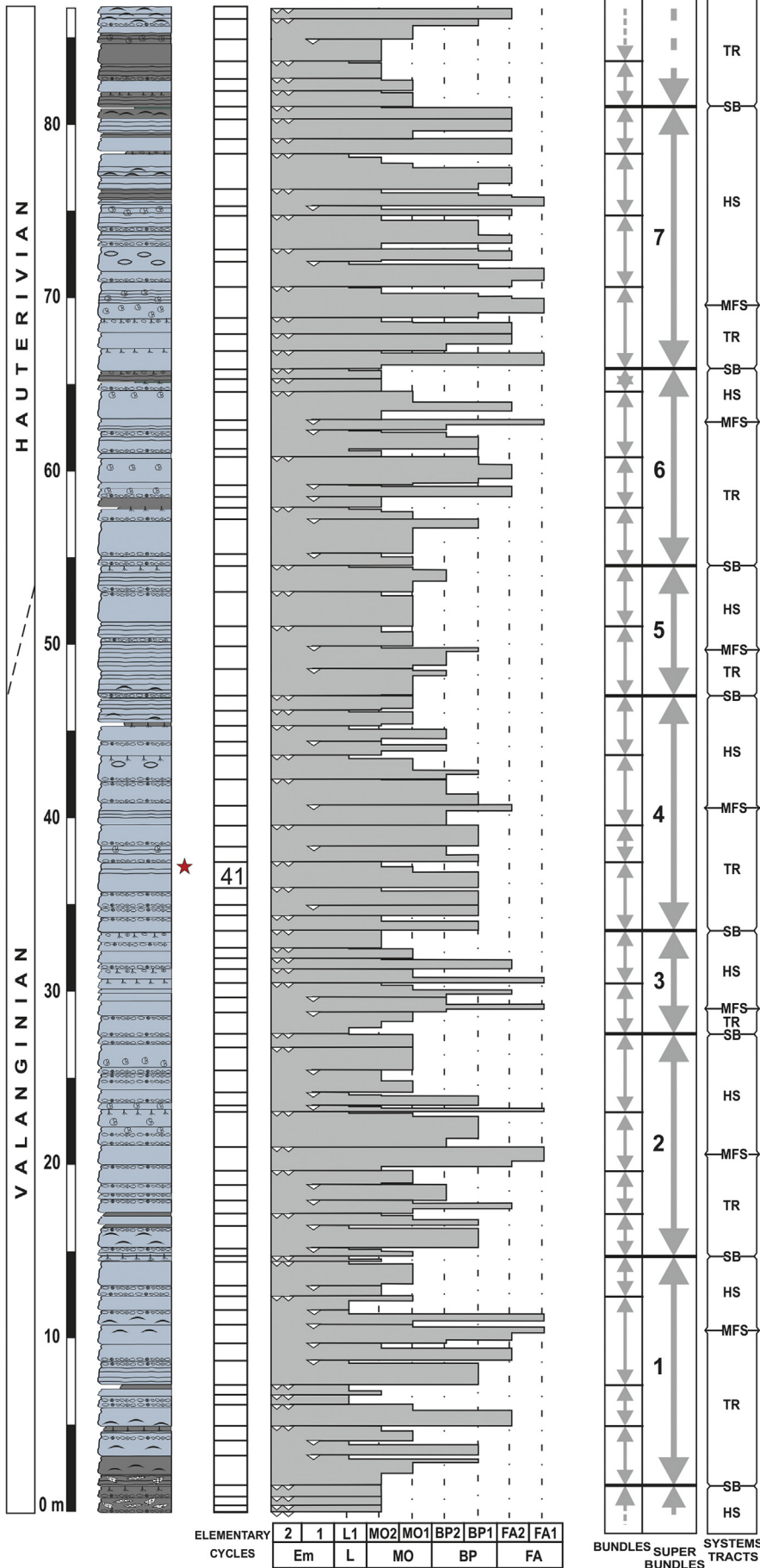
The carbonate dendritic structures have been recognized within a single horizon, about 30 cm thick. They occur sporadically at a level near the top of elementary cycle 41 (Fig. 3, see Amodio, 2006; Amodio et al., 2008b). Based on previous biostratigraphic studies, the age of these deposits is Late Valanginian (about 135 Ma).

The carbonates at this horizon are wackestone and wackestone-packstone with miliolids, textularids, and ostracods. Less common *Hedstroemia*-group, nerineid gastropod, bivalve, and dasycladalean (*Salpingoporella annulata*) fossils also occur. Peloids are very abundant in the matrix. The overall biotic associations of these deposits are typical of marginal-marine environments, consistent with innermost shallow lagoon and ephemeral tidal/supratidal settings. In previous studies, this lithofacies was codified “MO2” and included in the “Mili-Ostracod limestones” lithofacies association (Fig. 2, see also Tab. 1, p. 56, in Amodio, 2006).

The dendritic fabric occurs within fenestral cavities (Fig. 4) in the upper part of a weakly laminated horizon. The fenestrae are roughly concordant with the stratification and include irregularly distributed keystone vug and birdseye structures. These cavities appear to have been variously formed by desiccation, gas bubbles, burrows and soft sediment deformation. The internal sediment of the cavities is commonly fine grained (micrite, or laminated silt), and locally contains ostracods and peloids (Fig. 5a). The fenestral cavities are millimeter to centimeter in size, and appear to have been irregularly enlarged by meteoric waters during emersion of the platform. Lowering of the sea level, even by just a few meters, produced a subaerial discontinuity. The lithified surface created by early cementation shows borings and discoloration (Fig. 5b, Amodio, 2006). Evidence of meteoric-vadose diagenesis and karstic features immediately below this surface extends downwards for several tens of centimeters. We observed no signs of pedogenesis, but pervasive dissolution indicated by karstic cavities with geopetal crystal silts and botryoidal cements is evident (see Section 6).

5. Description of carbonate dendritic fabric

The dendritic structures have only been observed within microkarstic cavities and typically occur within botryoidal cements (Fig. 5c–f). Individual San Lorenzello dendrites are typically densely micritic sub-millimetric masses (typically 50–300 μm in size) with distinct highly irregular margins. They show distal elongation and



Legend

Mineralogy

- Marls and/or clay
- Dolomite
- Limestone

Symbols

- Sarmenofascis?
- Bivalve shells
- Requieridae
- Ostreidae
- Tempestite
- Stylolites
- Calcrete

Lithofacies Associations:

- FA: For-Algal limestones (open lagoon)
- BP: Bio-Peloidal limestones (sandy shoals)
- MO: Mili-Ostracod limestones (restricted lagoon)
- L: Laminated limestones (tidal plain)

Emersion surfaces:

- Em1-type: microkarst and/or weak pedogenesis
- Em2-type: Paleokarst and/or paleosol

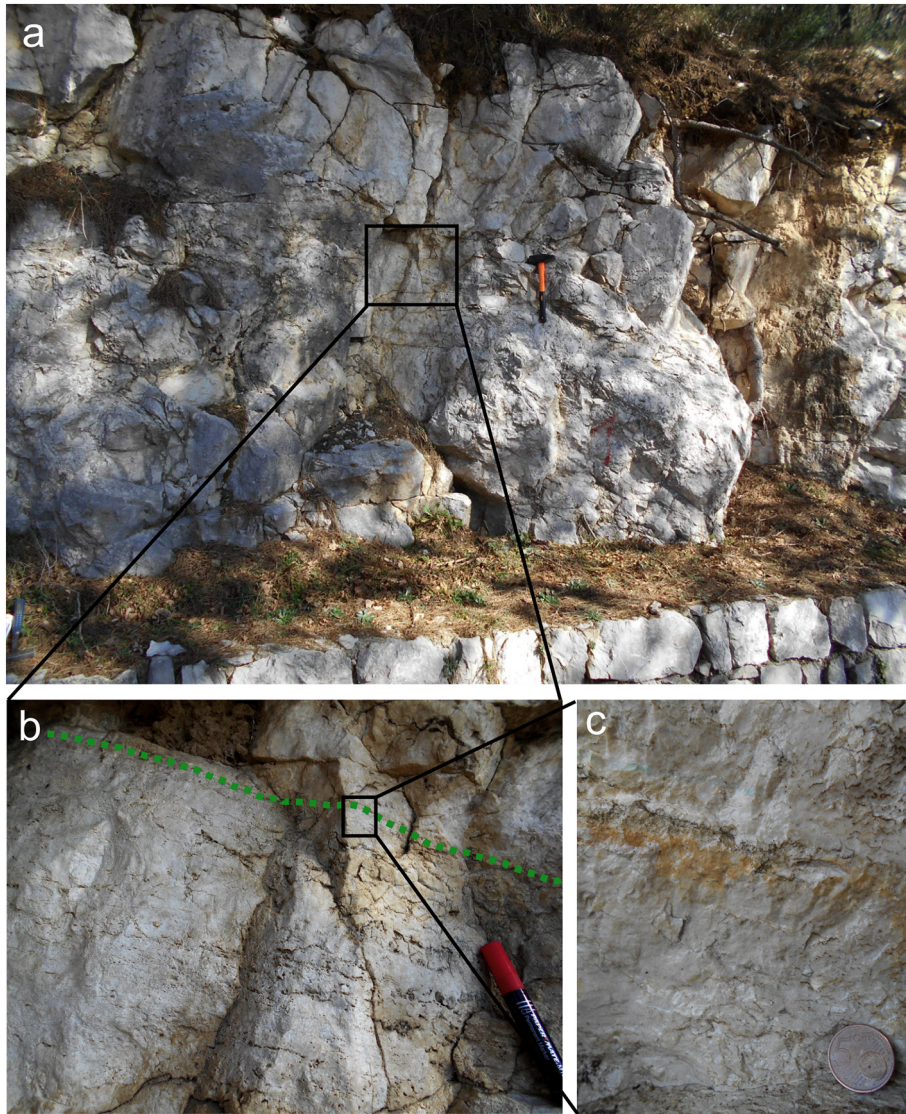


Fig. 3. San Lorenzello outcrop details. (a) Panoramic view of the strata, which correspond to the elementary cycle 41. (b) Detail of the topmost part of cycle 41, showing slightly laminated horizon with fenestral fabric. Green dashed line marks the subaerial discontinuity. (c) Detail of (b) showing the stylolite horizon where the dendritic structures described here occur. (For interpretation of the references to color in this figure, the reader is referred to the web version of this article.)

expansion, and often develop broad inflated branches that produce shrub-like masses ranging from compact and squat, to elongate and dendritic in shape (Fig. 5c). They occur in dense masses and clusters, generally oriented perpendicular to cavity surfaces, surrounded by sparry cement. This superficial simplicity is complicated by a tendency for filaments to be almost fractal and have margins that are highly irregular. This appearance is produced by linearly arranged, almost discontinuous, irregularly radial bush-like masses, ~100–200 μm across, within which smaller divergent filaments ~50 μm wide are present. The fabric is entirely micritic and no tubes have been observed. Dendritic fabric tends to grow centripetally within the cavities (Fig. 5d). The filaments are mainly pendent (Fig. 5e), but also develop laterally or on cavity floors (Fig. 5f). The cements appear to support (Fig. 6a) and/or partially envelope the dendrites. In some cases, the dendrites also appear to have grown on micritic surfaces and are evident at the micrite/cement interface (Fig. 6b). Evidence of dendritic fabric surrounded by micrite has been not observed.

6. Diagenetic processes and cementation

Three types of cement (using terminology of Flügel, 2004) are commonly associated with the dendritic masses in these cavities.

1. Gray granular micritic-microsparitic cement that occurs in three ways:
 - a) Laminated thick crusts and dripstone (Fig. 6c). Light laminae appear coarser grained than dark ones (Fig. 6d). Small protuberances of this cement (resembling 'embryonic dendritic fabric') enveloped by thin yellow cement, occur rarely.
 - b) Narrow downward directed structures enveloped by thin yellow cements (Fig. 6e) occur rarely. These narrow structures appear primary.
 - c) Filling spaces between the branches of dendritic fabric. These relatively fine-grained crystals appear to be slightly later than the dendritic fabric, and typically completely envelope the branches with a 20–50- μm wide rim (Fig. 6f).

Fig. 2. Sedimentological log of the San Lorenzello section. The red star at the top of cycle 41 indicates the horizon with dendritic fabrics described here. Sedimentary cyclicity, as elementary cycles, bundles (group of elementary cycles) and superbundles (group of bundles), and sequence stratigraphic interpretation are modified from Amodio (2006). (For interpretation of the references to color in this figure legend, the reader is referred to the web version of this article.)

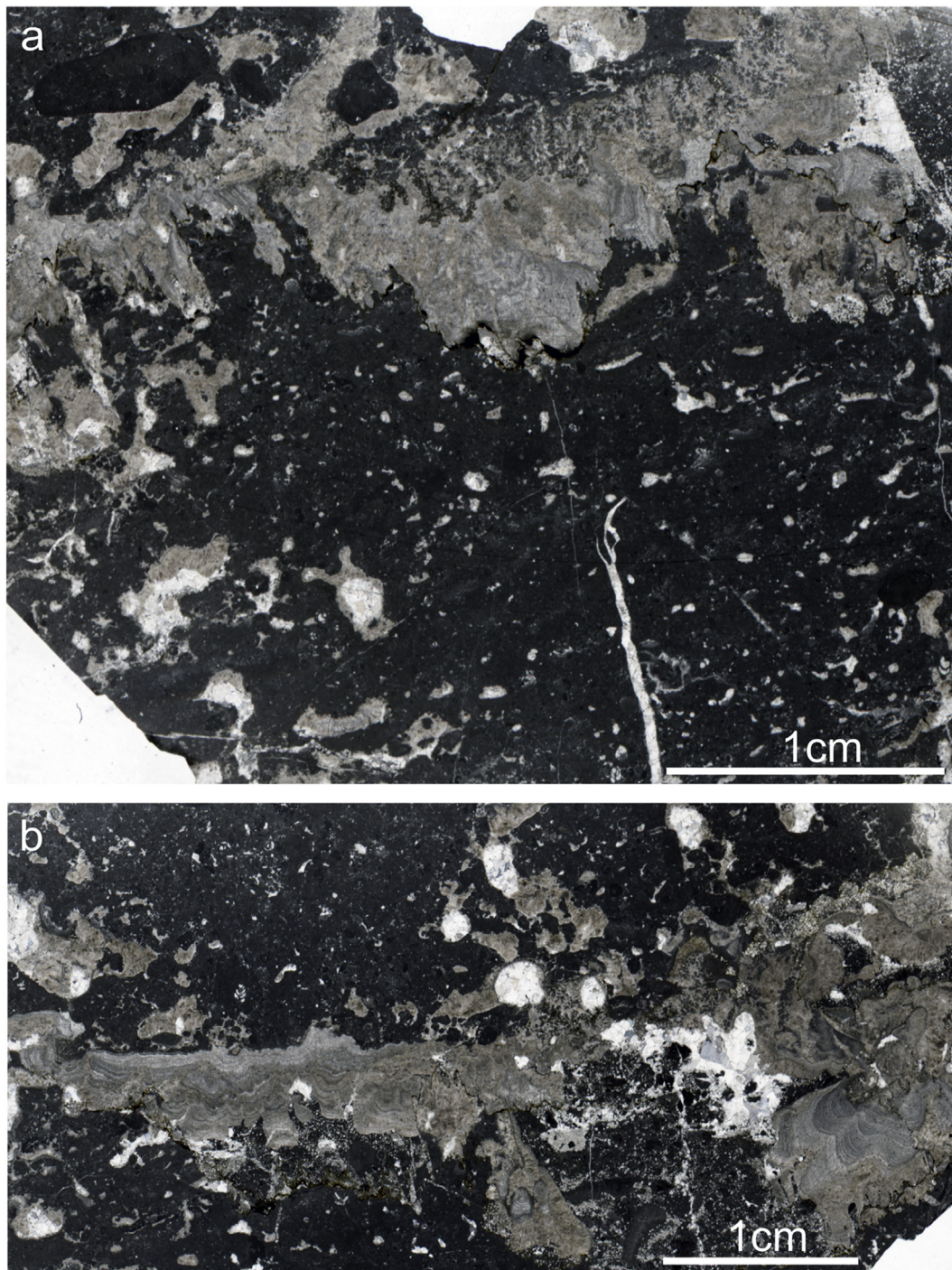


Fig. 4. Mili-Ostracod wackestone-mudstone (dark gray) containing irregular cavities (light gray) filled by cements enclosing dendritic fabric. (a) Pendent dark micritic dendritic fringes at the top of an enlarged microkarstic cavity that corresponds to the main subaerial discontinuity. The dark mudstone shows the micro-fenestral fabric, typical of tidal-supratidal settings; thin section 46/47.1, positive print; (b) similar view showing the relatively flat-top of a centimeter microkarstic cavity (center left) and layered pendent botryoidal cements (lower right); thin section 46/47.2, positive print.

2. Yellow crustose to dripstone cement

- a) Fountain-like/zoned cements form large gravitational botryoidal to zoned dripstone layers and appear yellow and fibrous (Fig. 7a and b). No dendrites have been found within them, but extraneous particles are rarely present. This generation appears to be distinct from Type 1, presumably due to different chemical conditions.
- b) Yellow radiaxial cement. This forms large unlaminated gravitational crusts and dripstone with large crystals (Fig. 7c). In other respects, it resembles Type 2a.

3. Drusy cement. This filled residual voids during the last phase of cementation. It is juxtaposed with Type 1b, 2a and 2b cements (Fig. 7d).

6.1. Interpretation

The horizon containing the cavities with dendritic fabric shows evidence of dissolution, cementation, compaction and pressure solution, as well as dolomitization. Intense early dissolution of

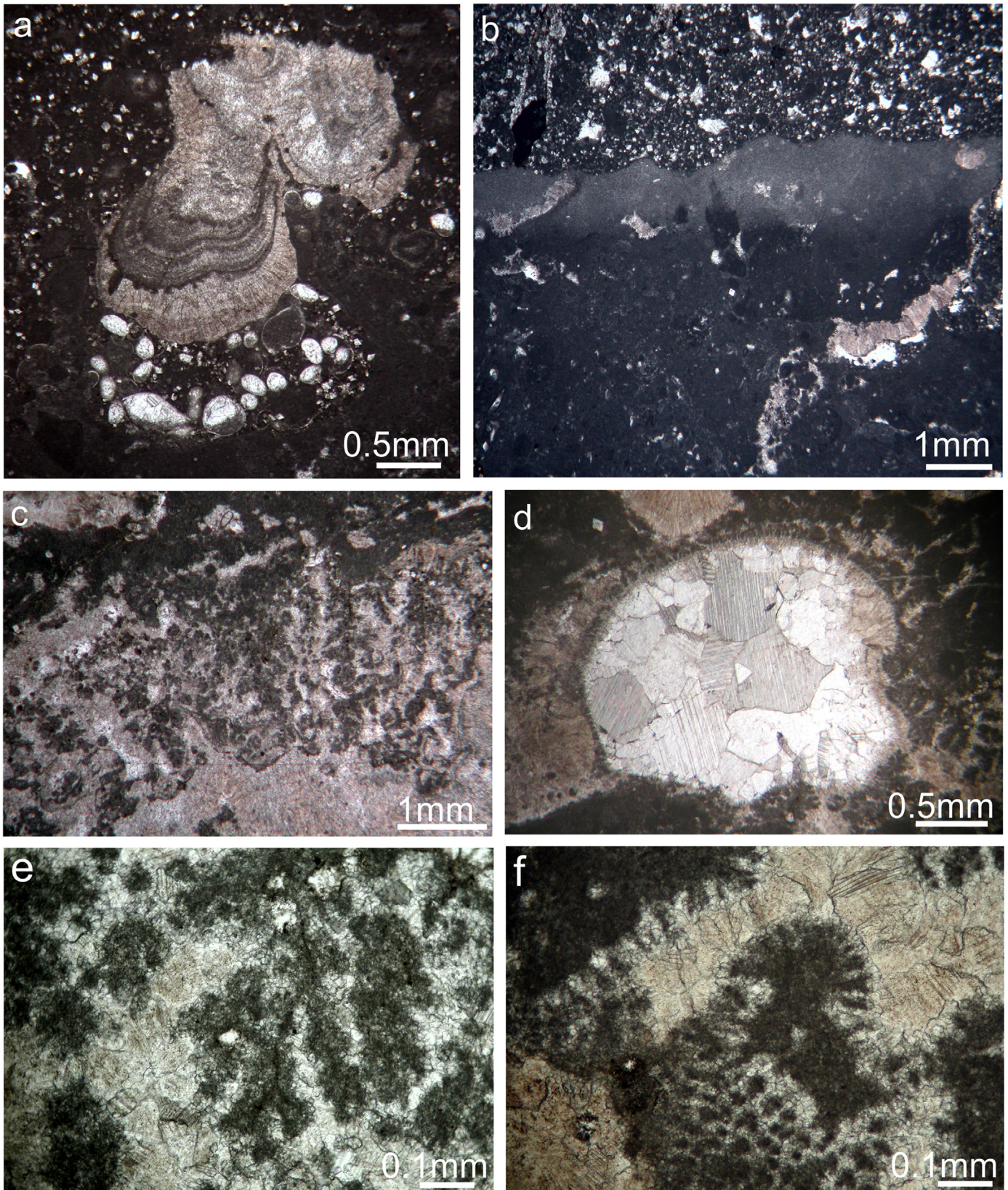


Fig. 5. (a) Close-up view of a microkarstic cavity filled by micrite with ostracod shells at the base and granular micritic-microsparitic laminated crust and radiaxial cement at the top; thin section Ba.4411.b.1, positive print; (b) detail of the discontinuity surface at the top of cycle 41, characterized by bioerosion and discoloration. The microcavities display geopetal fillings characterized by fibrous radiaxial pendent cements; thin section Ba.4411.b.1, positive print; (c) micritic dendritic shrub-like masses showing downward branching growth pattern within a microkarstic cavity; thin section 46/47.1, positive print; (d) embryonic dendritic fabric that grew centripetally around a cavity subsequently occluded by drusy calcite; thin section 46/47.2, positive print; (e) detail of (c) showing the pendent micritic filaments. (f) Another detail of thin section 46/47.2 showing the highly organized cauliflower-like shape of the dendritic fabric, growing upward from the cavity floor.

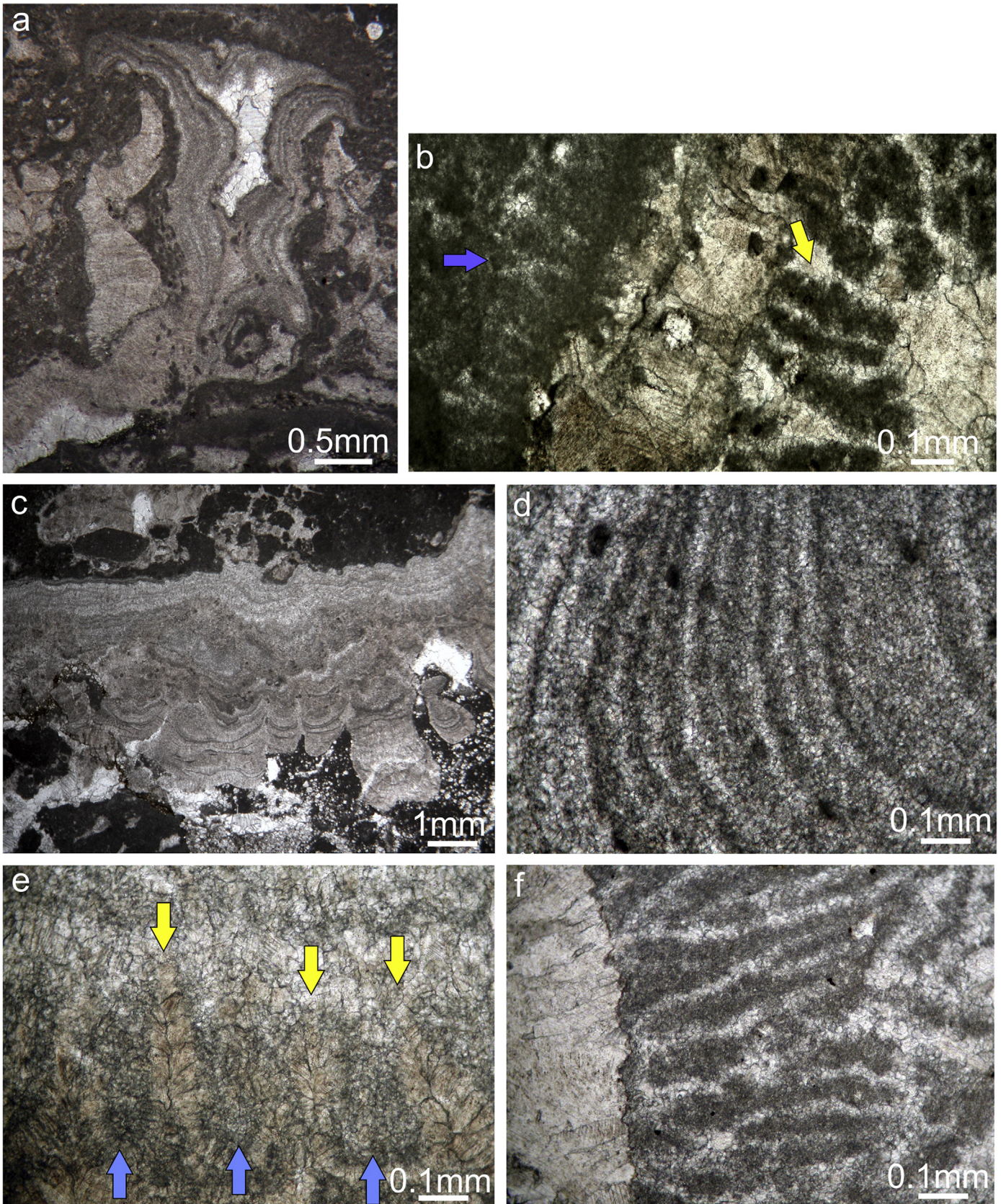


Fig. 6. Micritic dendritic fabric. (a) Two generations of dendritic fabric separated by cement crusts; thin section Ba.4411.c.2, positive print; (b) a first generation of dendrites grows on a micritic substrate (blue arrow) while the second generation (yellow arrow) nucleates on yellowish radiaxial cements; thin section 46/47.2, positive print; (c–f) examples of different types of cement associated with the micritic dendrites. (c) Laminated crust with light and dark millimetric bands of gray granular cement displaying wavy contours with local fan-like crystal clusters. The lamination is related to micritic-microsparitic changes in crystals size. Thin section 46/47.2, positive print; (d) detail of banded granular cement. Thin section 46/47.2, positive print; (e) detail showing downward growth pattern of the granular cements (blue arrows) surrounded by yellow radiaxial cements (yellow arrows). Thin section 46/47.2, positive print; (f) detail of sub-horizontal micritic branches enclosed by a rim of microsparite crystals. Thin section 46/47.2, positive print. (For interpretation of the references to color in this figure, the reader is referred to the web version of this article.)

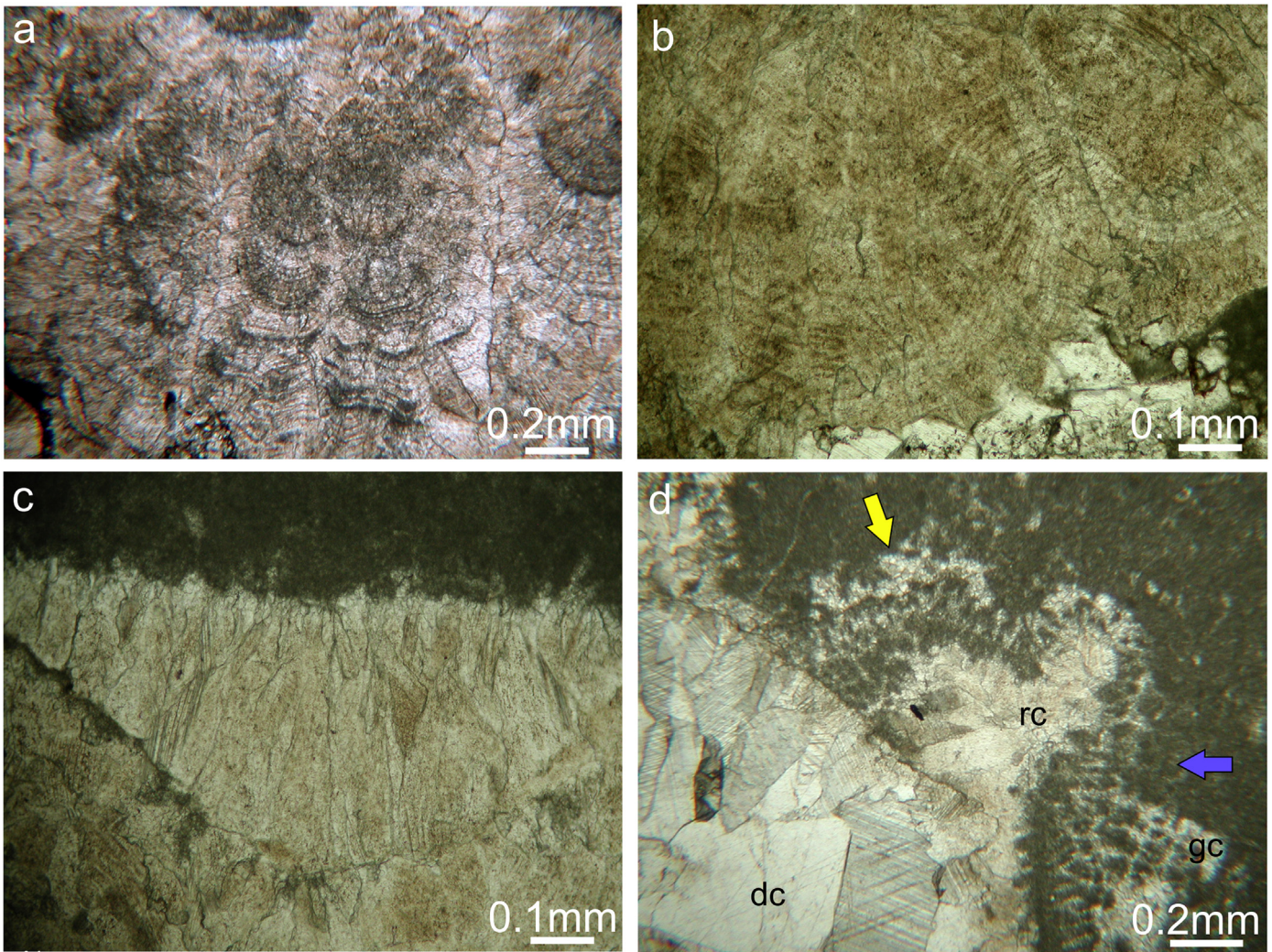


Fig. 7. Examples of arrangement of cement crystals. (a) Close-up view of zoned dripstone fabric consisting of coalescing millimeter-size mamelons made of densely packed yellow fibrous crystals radiating downwards into a cavity. Thin section 46/47.2, positive print; (b) detail of banded fan-like fibrous cement. Thin section 46/47.2, positive print; (c) relatively coarse pendent fringes of yellowish radiaxial calcite cement, filling a cavity. Thin section 46/47.1, positive print; (d) close-up view showing three types of cements progressively filling a cavity: granular cement (gc), radiaxial cement (rc), drusy cement (dc). The micritic dendrites between gc and rc grow centripetally on micrite (blue arrow) as well as on granular cement (yellow arrow). Thin section 46/47.2, positive print. (For interpretation of the references to color in this figure, the reader is referred to the web version of this article.)

matrix was followed by widespread production of crystal silt. Syndimentary small cavities (fenestrae) were irregularly enlarged in very shallow meteoric environments. Cementation resulted in the precipitation of several generations of cement within these cavities

due to successive fluid circulation. Granular and radiaxial calcite arranged as botryoidal and pendent structures locally form thick dripstone-like crusts. Drusy mosaic cements infilled remaining spaces.

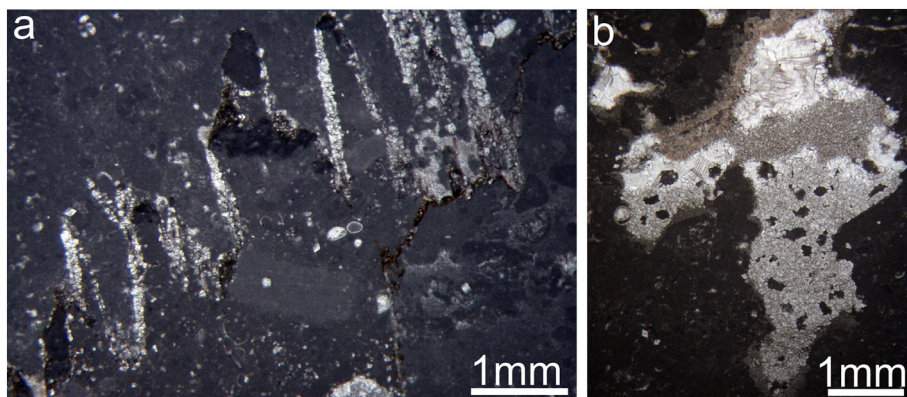


Fig. 8. Burial dolomite in the topmost part of cycle 41. (a) Stylolite characterized by concentration of insoluble clay residues together with dolomite that appears to be a selective replacement of calcite. Thin section BA4411.b.4, positive print; (b) two generations of dolomite: the first one with a coarse mosaic groundmass produced by partial replacement of micritic cavity filling; the second appears as an upper fine-grained mosaic. Thin section BA4411.b.4, positive print.

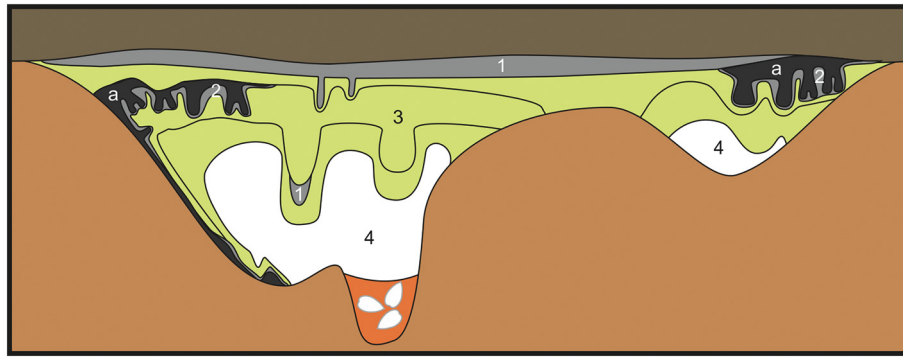


Fig. 9. Sketch illustrating relationships between dendritic fabric (a), and the four generations of cement described in the text: 1) granular cement forming laminated crusts and fringes; 2) isopachous granular coatings around micritic dendritic fabrics; 3) layered dripstone with yellow radial and fibrous fountain-like fabrics; 4) drusy mosaic. (For interpretation of the references to color in this figure, the reader is referred to the web version of this article.)

Subsequent compaction and pressure solution generated stylolites that partially obliterated the discontinuity surface at the top of the cycle 41 and reduced the underlying karstified horizon (Fig. 4).

Dolomitization appears to postdate stylolitization as dolomite crystals follow these sutures and appear to replace geopetal silt in the karstic cavities (Fig. 8).

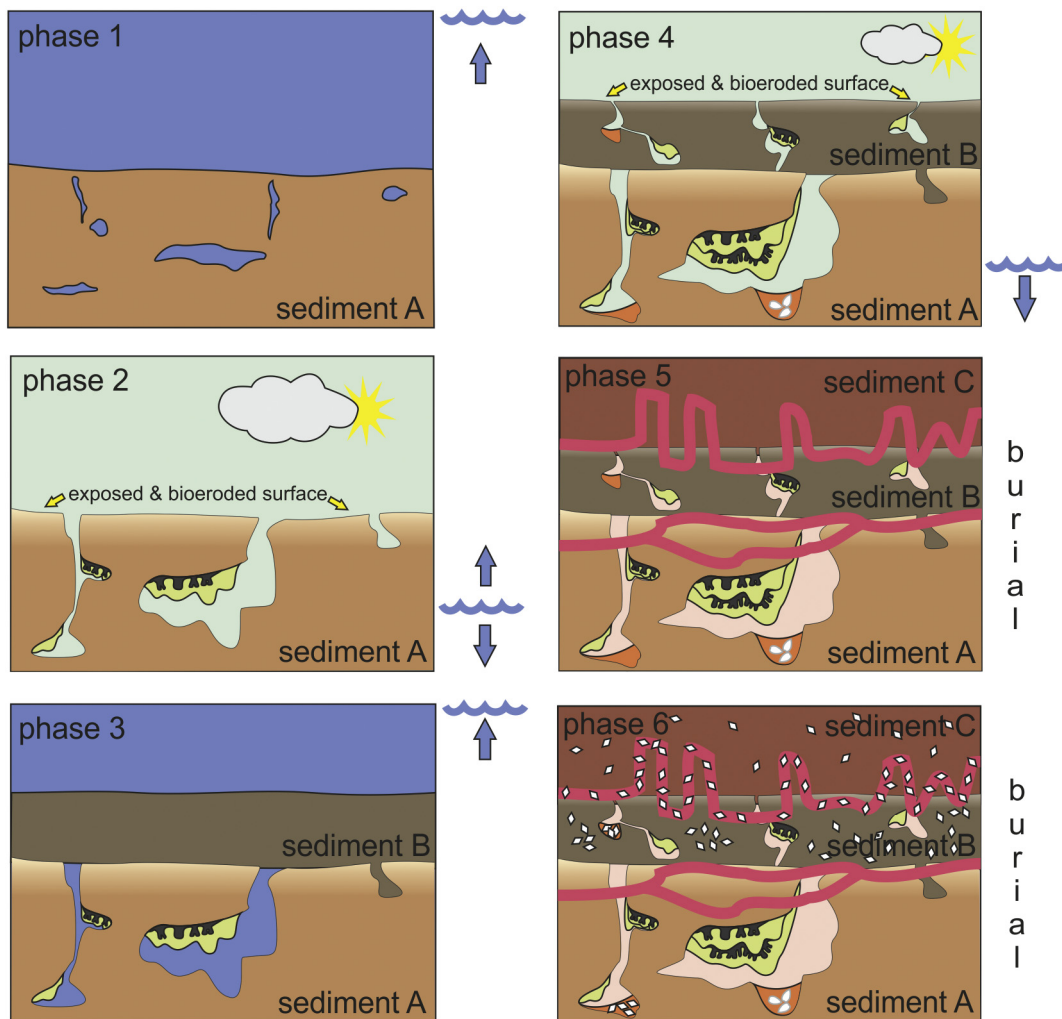


Fig. 10. Line drawings illustrating the sequence of depositional and diagenetic phases (1 to 6) through time. 1: Peritidal deposition of muddy fenestral carbonate (sediment A). 2: Sea level fall exposes sediment A to bioerosion and microkarstification which enlarges vugs and a first generation of dendritic fabric develops, followed by precipitation of enclosing gray granular and then yellow radial cement. 3: Sea-level rise submerges the surface and deposits a new layer of muddy carbonate (sediment B) which partially infills the cavities in sediment A. 4: Repetition of sea level fall, exposing sediment B (corresponding to the top of cycle 41) to subaerial exposure, bioerosion and karstification. New cavities form, earlier ones are enlarged, and sea level oscillation results in alternating percolation of marine and freshwater. A second generation of dendritic fabric and associated cements form in the cavities. 5: Multiphase iteration of sea-level rise and fall result in renewed sediment accumulation (sediment C and additional layers) and karstic episodes. Drusy mosaic cement (pink) occludes remaining cavities. This phase includes later progressive burial, resulting in dewatering, compaction and ultimately stylolitization, as observed at the top of the elementary cycle 41. 6: Dolomitization postdates stylolitization. (For interpretation of the references to color in this figure, the reader is referred to the web version of this article.)

Overall, dissolution and cementation products mainly appear to have occurred during marine-vadose and meteoric-vadose diagenesis. Stylolitization and dolomitization developed during the burial phase.

7. Discussion

Based on the relationships between the micritic dendritic masses and their associated cements we recognize an early generation of dendritic fabric that nucleated on micritic cavity surfaces, and a later generation (possibly several generations) that developed within granular as well as radiaxial cements (Fig. 9). Since the dendritic fabric usually occurs centripetally within the cavities, the filaments expand downwards as asymmetric fringes (Figs. 4a and 5c) but also grow horizontally (Fig. 6a, b and f) and upwards (Fig. 5f). The preservation of the dendritic fabric appears to be closely related to the conditions within the cavities, as discussed in the following section. The micritic composition, and the growth pattern displaying irregular morphologies of branches characterized by the close relationships with Cement Type 1, could suggest a biotic origin for the dendritic fabric, but abiotic origins and influences cannot be excluded, especially in relation to the cement encasing the micritic dendrites (e.g., Chafetz, 2013). We discuss these possibilities by comparing a variety of calcimicrobes (from marine and freshwater environments) and travertine shrub morphotypes.

7.1. Diagenetic pathway and model of development

Based on details of the dendritic fabric and cements, and the overall depositional and diagenetic history of these deposits, we propose the following model to describe the sequence of events (sedimentation, lithification, dissolution, erosion, cementation) and their interactions (Fig. 10).

- Phase 1 Deposition of peritidal muddy carbonate sediment A. Millimetric fenestral cavities (keystone vugs, birdseyes) form during episodic phases of desiccation that consolidate and early lithify the mud (sediment A, Fig. 10). *Environment*: shallow water, subtidal/intertidal.
- Phase 2 Sea level fall exposes sediment A to bioerosion and microkarstification (Fig. 10). The vugs and cavities are enlarged by dissolution. Minor sea level oscillations induce episodic percolation of alternately marine and relatively fresh water. A first generation of dendritic fabric develops, followed by precipitation of enclosing gray granular and then yellow radiaxial cement. *Environment*: mixing water, tidal/supratidal.
- Phase 3 Sea-level rise submerges the surface and a new layer of muddy carbonate sediment is deposited (sediment B, Fig. 10). The texture and biota of these sediments are similar to those of sediment A, but also include radial fibrous ooids. Sediment B fills the bioerosion and other cavities within sediment A. *Environment*: shallow water, subtidal.
- Phase 4 Sea level falls and the deposits are subaerially exposed again. A second phase of bioerosion and karstification takes place (Fig. 10). The top of sediment B (corresponding to the top of elementary cycle 41) is exposed and experiences bioerosion. Simultaneously, karstification forms new cavities in sediment B and enlarges those previously developed in the sediment A. Sea level oscillations result in alternating percolation of marine to freshwater solutions. A first generation of dendritic fabric forms in sediment B, together with precipitation of gray granular, followed by yellow radiaxial, cement. A second generation of dendritic fabric and associated cement forms in the cavities of sediment A. *Environment*: mixing water, tidal/supratidal.

Phase 5 Iteration of sea-level rise and fall results in renewed sediment accumulation (sediment C and additional layers) and karstic episodes (Fig. 10). Drusy mosaic cements (pink area) occlude remaining cavities. This phase is multiphase and also includes later progressive burial. Overall, it results in dewatering, compaction and ultimately stylolitization, as observed at the top of the elementary cycle 41. Stylolitization appears to partially cut and obliterate the fabric created during the previous 1–4 phases.

Phase 6 Dolomitization postdates stylolitization. Euhedral dolomite crystals form in sediment B and C, and along stylolites (Figs. 8a and 10). Granular dolomite locally replaces geopetal silt in cavities (Fig. 8b).

7.2. Comparisons

San Lorenzello dendritic fabric can be compared with a wide variety of deposits (Fig. 11), from freshwater calcified cyanobacteria (Riding and Voronova, 1982) and similar Paleozoic microfossils, to hot spring travertine shrubs, which also can be surrounded by clear sparite (Claes et al., 2017). However, San Lorenzello fabrics are essentially pendent (Fig. 11a and b). In this respect they appear to differ from most hot spring shrubs, whereas some similar Paleozoic fossils can be pendent within reef cavities (Pratt, 1984).

7.2.1. Paleozoic calcimicrobes

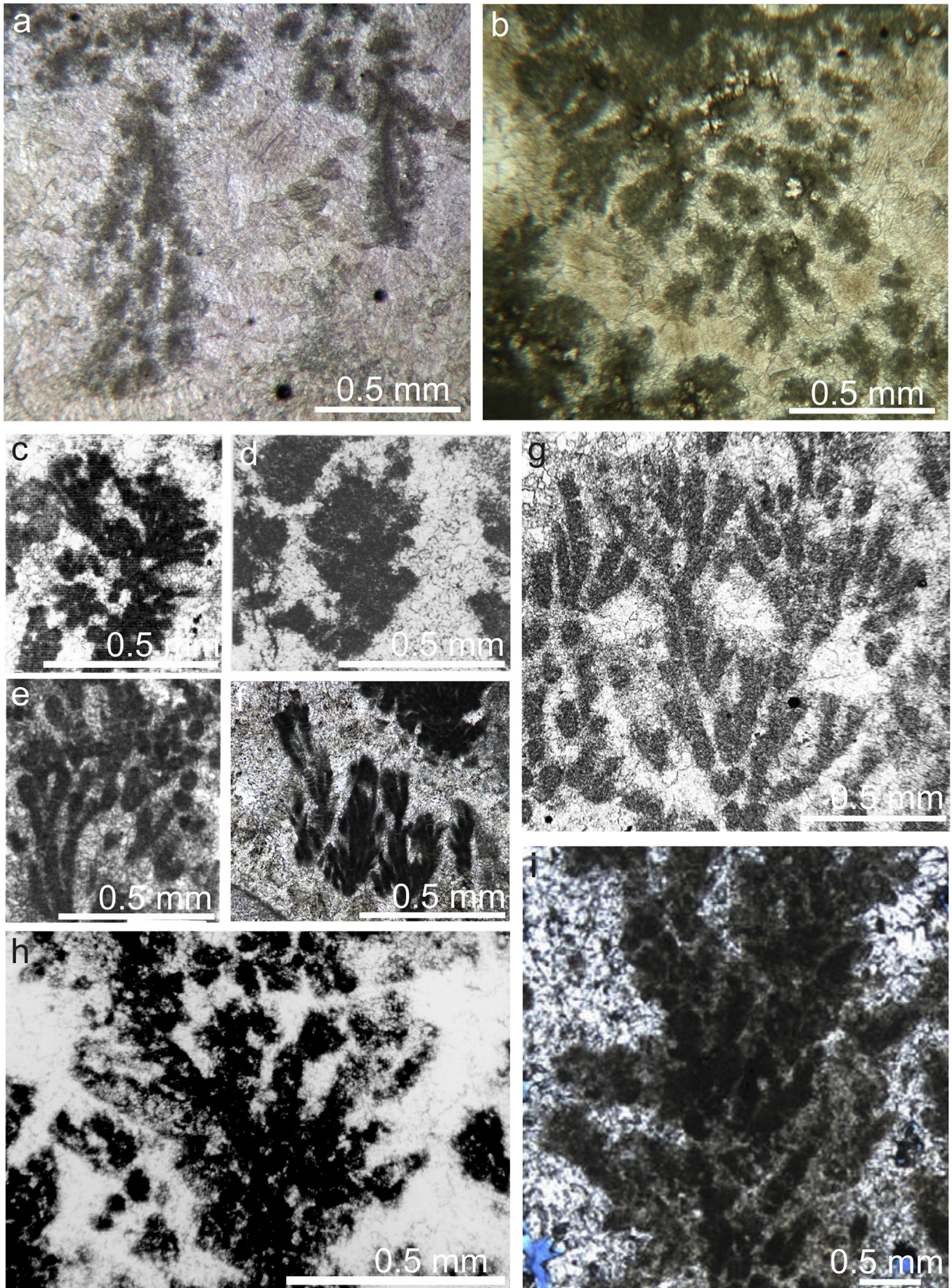
The small dendritic calcified fossils *Epiphyton*, *Renalcis* and *Angusticellularia* are common components of Early Cambrian reefs (Figs. 11d, e and g; Riding and Voronova, 1982; Pratt, 1984; Woo et al., 2008). *Epiphyton* and *Renalcis* are of uncertain affinity, but *Angusticellularia* appears to have a present-day analogue in freshwater cyanobacteria (Riding and Voronova, 1982). *Epiphyton* has also been compared with present-day lacustrine carbonate fabrics (Laval et al., 2000). *Renalcis* is a distinctly chambered fossil, and in this respect clearly differs from San Lorenzello dendrites. In contrast, some *Epiphyton* (Figs. 11c and e), and especially *Angusticellularia*, show closer similarities with San Lorenzello dendrites (Fig. 11a and b).

7.2.1.1. *Epiphyton*. Epiphytaceans typically have narrow elongate smooth dendritic to dichotomous branches, often characterized by long relatively narrow smooth sided and dichotomously branched filaments up to 1 mm in length (Korde, 1958). Some are reported to be pendent (Riding, 1991a). In contrast, San Lorenzello shrubs are generally much shorter, squat and irregular and on close inspection appear to consist of smaller, divergent sub-dendrites. Nonetheless, although they generally have a much less regular structure than most epiphytaceans, there are some resemblances between San Lorenzello shrubs and short segments of *Epiphyton*.

7.2.1.2. *Angusticellularia*. In size and shape, San Lorenzello dendrites quite closely resemble extant lacustrine calcified cyanobacterial analogs of the Cambrian fossil *Angusticellularia/Angulocellularia* in Canandaigua Lake, New York State (Fig. 11d; Riding and Voronova, 1982). San Lorenzello shrubs are broadly similar in size and shape to Canandaigua *Angusticellularia*, forming dense irregularly elongate crudely branched/expanding shrub-like masses with very irregular margins a few 100 μm in size.

7.2.2. Kimmeridgian-Tithonian fossils

Dendritic fossils from the Late Jurassic of Romania that occur surrounded by sparry calcite, in marine reefs (Fig. 11f; Săsăran et al., 2014), resemble *Epiphyton*, but are unlike San Lorenzello micritic sub-dendrites. They are associated with segmented dendritic fossils somewhat similar to Cretaceous *Sgrossoella* (De Castro, 1969) or Permian *Gahkumella* (Zaninetti, 1978). These are larger, more elongate, and



less irregular (Fig. 11f) than most San Lorenzello micritic shrubs (Fig. 11a and b), as well as being composed of arcuate juxtaposed bowl-like segments.

7.2.3. Quaternary travertine shrub fabric

San Lorenzello dendrite fabric resembles some hot spring travertine shrub fabric in shape, e.g., Tivoli, Italy (Fig. 11i; Della Porta, 2015; Anzalone et al., 2017; Della Porta et al., 2017; Erthal et al., 2017), but is generally smaller, typically 1/4–1/2 of the size. In contrast, shrubs from Mammoth Hot Springs resemble San Lorenzello fabric in both size and shape (Fig. 11h; Chafetz and Guidry, 1999). They are surrounded by sparry cement, as are shrubs figured by Erthal et al. (2017). The origins of travertine shrubs remain uncertain. A bacterial origin has been suggested (Chafetz and Folk, 1984), and travertine shrub fabrics have previously been compared with Paleozoic fossils such as *Epiphyton* and *Renalcis* by Chafetz and Guidry (1999). On the other hand, crystal shrubs have often been regarded as abiotic (Pentecost, 1990; Chafetz and Guidry, 1999; Gandin and Capezzuoli, 2014). The formation of some travertine shrubs has been attributed to a combination of biotic and abiotic processes (Guo and Riding, 1994).

8. Assessment

Based on these comparisons, morphologically San Lorenzello shrub fabric most closely resembles extant calcified cyanobacteria similar to Paleozoic *Angusticellularia* (Fig. 11d; Riding and Voronova, 1982; Riding, 1991b), and also to some Quaternary travertine shrubs (Fig. 11h, i). San Lorenzello fabrics appear to have formed in microkarst cavities.

Although a cyanobacterial origin is possible, an abiotic origin might appear more likely in this microkarst setting – even though it is well-known that cyanobacteria can grow in low light conditions (Gan and Bryant, 2015). Carbonate shrub-like (Fig. 2 in Jones and Motyka, 1987; Martín-García et al., 2011) and opaline dendritic (e.g., López-Martínez et al., 2016) speleothem fabrics occur on open cave surfaces. However, the only shrub-like structures we are aware of, that line small cavities and closely resemble San Lorenzello shrubs, occur in karst breccia filling a sinkhole within Miocene dolostones on the Cayman Islands, and have been interpreted as microstromatolites produced by detrital micrite trapped and bounded by filamentous microbes (Figs. 6 and 8 in Jones and Kahle, 1995). Shrub-like morphologies in stromatolitic lithofacies have been documented in sub-Recent ambient water travertines at Pontecagnano (southern Italy, Anzalone et al., 2007) where a microbial origin has been suggested. On the other hand, we are not aware of pendent examples of shrubs in hot spring fabrics.

Evaluating similarities based on these observations is challenging. These fabrics and microfossils are relatively simple, and their resemblance could be superficial. We cannot unequivocally resolve their process of formation. Two generations of micritic shrub in the same cavity can be originated by organically and/or inorganically mediated processes that could have operated in different ways through time. San Lorenzello dendritic fabric shows similarities with a variety of both Paleozoic and Mesozoic marine microfossils, as well as with shrub-like fabrics found in Quaternary travertine deposits. We cannot exclude the possibility that these fabrics are essentially abiotic; this would be consistent with their cryptic occurrence within pendent dripstone cement fabrics and with their local rather regular spacing and appearance.

D'Argenio and Ferreri (2004) suggested that hot water travertines show a decrease in abundance, diversity and size of colonizing organisms with respect to ambient waters ones (see also Pentecost, 2005; Capezzuoli et al., 2014). In other words, the chemistry and the temperature of hot water springs promote rapid carbonate precipitation but tend to inhibit the growth of most microbes (Dupraz et al., 2009; Konhauser and Riding, 2012). If lithofacies diversity and biogenic imprint on primary travertine texture are reliable criteria to distinguish ambient from hot water travertines, this could support a biotic origin for the San Lorenzello shrub-like structures, because in this case we can exclude the possibility that they precipitated in a hot water system.

Further studies need to distinguish depositional and diagenetic origins of the micritic fabrics, as well as more detailed morphological comparisons with extant analogs, in order to shed light on the formation of these distinctive deposits.

9. Conclusions

San Lorenzello Valanginian cryptic dendritic fabrics consist of numerous juxtaposed mainly pendent shrub-like micritic masses encased in spar within microkarstic cavities, closely associated with dripstone cements. They probably formed during early meteoric diagenesis within desiccation cavities produced by early lithification and later enlarged by meteoric waters during the emersion phase of the platform. Based on comparisons with a variety of contrasting deposits, from freshwater calcified cyanobacteria and similar Paleozoic microfossils, to hot spring travertine shrubs, San Lorenzello dendritic fabric resembles extant freshwater calcified cyanobacteria that have been compared with the Paleozoic fossil *Angusticellularia*, but also resembles some Quaternary hot-spring travertine shrubs. These similarities, together with their micritic composition, the irregular growth pattern of the branches and close relationships with surrounding granular cement, could favor a biotic origin for this dendritic fabric. However, an abiotic origin might appear more likely in view of the microkarstic setting and cryptic occurrence within pendent cement fabrics, as well as with the relatively regular spacing and appearance of these dendrites. Further studies and comparisons are required to shed light on the formation of these distinctive shrub-like fabrics.

Acknowledgements

S. Amodio was financially supported by Parthenope University (Bando Sostegno alla Ricerca individuale 2016–2018). F. Barattolo was funded by the DiSTAR Department, Federico II University (RDip. Progetto Unico 2018, prof. F. Barattolo). We thank Ioan Bucur and an anonymous reviewer, together with Brian Jones, for very helpful comments and suggestions that improved the final manuscript.

References

- Amodio, S., 2006. Foraminifera diversity changes and paleoenvironmental analysis: the Lower Cretaceous shallow-water carbonates of San Lorenzello, Campanian Apennines, southern Italy. *Facies* 52, 53–67.
- Amodio, S., Ferreri, V., D'Argenio, B., Sprovieri, M., Weissert, H., 2008a. Cyclostratigraphy and C-isotope stratigraphy of shallow-marine carbonates as proxies of climatic-paleoceanographic global changes. Case histories from Early Cretaceous of southern Italy. *Rendiconti Online della Società Geologica Italiana* 2, 9–12.
- Amodio, S., Ferreri, V., D'Argenio, B., Weissert, H., Sprovieri, M., 2008b. Carbon-isotope stratigraphy and cyclostratigraphy of shallow-marine carbonates. The case of San Lorenzello, Early Cretaceous of southern Italy. *Cretaceous Research* 29, 803–813.

Fig. 11. Comparisons between San Lorenzello dendritic fabric (a and b) and a variety of calcimicrobes and travertine shrubs (c–i). (c) *Epiphyton* in stromatoporoid reef (Devonian, Alberta), modified from Riding (1991b); (d) *Angulocellularia* in algal-archaeocyath bioherms (Cambrian, Mongolia), modified from Riding and Voronova (1982); (e) detail of *Epiphyton* branches in reef (Cambrian, Newfoundland) modified from Pratt (1984); (f) a specimen, resembling *Epiphyton* like fossils in coral-microbial reef (upper Jurassic, Romania), modified from Săsăran et al. (2014); (g) detail of *Epiphyton* bioherm (middle Cambrian, North China), modified from Woo et al. (2008); (h) bacterial shrub in travertine, modified from Chafetz and Guidry (1999); (i) shrub in travertine (Late Pleistocene, Tivoli, central Italy), modified from Erthal et al. (2017).

- Anzalone, E., Ferreri, V., Sprovieri, M., D'Argenio, B., 2007. Travertines as hydrologic archives: the case of the Pontecagnano deposits (southern Italy). *Advances in Water Resources* 30, 2159–2175.
- Anzalone, E., D'Argenio, B., Ferreri, V., 2017. Depositional trends of travertines in the type area of Tivoli (Italy). *Rendiconti Lincei Scienze Fisiche e Naturali* 28 (2), 341–361.
- Capezzuoli, E., Gandin, A., Pedley, M., 2014. Decoding tufa and travertine (fresh water carbonates) in the sedimentary record: the state of the art. *Sedimentology* 61, 1–21.
- Chafetz, H.S., 2013. Porosity in bacterially induced carbonates: focus on micropores. *American Association of Petroleum Geologists Bulletin* 97 (11), 2103–2111.
- Chafetz, H.S., Folk, R.L., 1984. Travertines: depositional morphology and the bacterially constructed constituents. *Journal of Sedimentary Petrology* 54, 289–316.
- Chafetz, H.S., Guidry, S.A., 1999. Bacterial shrubs, crystal shrubs, and ray-crystal shrubs: bacterial vs. abiotic precipitation. *Sedimentary Geology* 126, 57–74.
- Claes, H., Erthal, M.M., Soete, J., Özkul, M., 2017. Shrub and pore type classification: petrography of travertine shrubs from Ballik-Belevi area (Denizli, SW Turkey). *Quaternary International* 437, 147–163.
- Cook, M., Chafetz, H.S., 2017. Sloping fan travertines, Belen, New Mexico, USA. *Sedimentary Geology* 352, 30–44.
- D'Argenio, B., Ferreri, V., 2004. Travertines as self regulating carbonate systems. Evolutionary trends and classification. *Földtani Közlöny Budapest* 13 (2), 209–218.
- D'Argenio, B., Ferreri, V., Amodio, S., Pelosi, N., 1997. Hierarchy of high-frequency orbital cycles in Cretaceous carbonate platform strata. *Sedimentary Geology* 113, 169–193.
- D'Argenio, B., Ferreri, V., Amodio, S., 2011. Eustatic cycles and tectonics in the Cretaceous shallow Tethys. Central-Southern Apennines. *Italian Journal of Geosciences* 130, 119–127.
- De Castro, P., 1969. Su alcune tallofite del Mesozoico in Campania, stratigrafia e paleontologia. *Bollettino della Società dei Naturalisti in Napoli* 78, 87–167.
- Della Porta, G., 2015. Carbonate build-ups in lacustrine, hydrothermal and fluvial settings: comparing depositional geometry, fabric types and geochemical signature. In: Bosenec, D.W.J., Gibbons, K.A., Le Heron, D.P., Morgan, W.A., Pritchard, T., Vining, B.A. (Eds.), *Microbial Carbonates in Space and Time: Implications for Global Exploration and Production*. Geological Society, London, Special Publication 418, pp. 17–68.
- Della Porta, G., Croci, A., Marini, M., Kele, S., 2017. Depositional architecture, facies character and geochemical signature of the Tivoli travertines (Pleistocene, Acque Albule basin, central Italy). *Rivista Italiana di Paleontologia e Stratigrafia* 123 (3), 487–540.
- Dupraz, C., Reid, R.P., Braissant, O., Decho, A.W., Norman, S.R., Visscher, P.T., 2009. Processes of carbonate precipitation in modern microbial mats. *Earth Science Reviews* 96, 141–162.
- Erthal, M.M., Capezzuoli, E., Mancini, A., Claes, H., Soete, J., Swennen, S., 2017. Shrub morphotypes as indicator for the water flow energy – Tivoli travertine case (Central Italy). *Sedimentary Geology* 347, 79–99.
- Ferreri, V., D'Argenio, B., Amodio, S., Sandulli, R., 2004. Orbital chronostratigraphy of the Valanginian-Hauterivian boundary. A cyclostratigraphic approach. In: D'Argenio, B., Fischer, A.G., Premoli Silva, I., Weissert, H., Ferreri, V. (Eds.), *Cyclostratigraphy. Approaches and Case Histories*. SEPM (Society for Sedimentary Geology) Special Publication 81, pp. 153–166.
- Flügel, E., 2004. *Microfacies of Carbonate Rocks. Analysis, Interpretation and Applications*. Springer-Verlag, Berlin Heidelberg.
- Fraiser, M.L., Corsetti, F.A., 2003. Neoproterozoic carbonate shrubs: interplay of microbial activity and unusual environmental conditions in post-snowball earth oceans. *Palaios* 18, 378–387.
- Gan, F., Bryant, D.A., 2015. Adaptive and acclimative responses of cyanobacteria to far-red light. *Environmental Microbiology* 17 (10), 3450–3465.
- Gandin, A., Capezzuoli, E., 2014. Travertine: distinctive depositional fabrics of carbonates from thermal spring systems. *Sedimentology* 61, 264–290.
- Golubić, S., Violante, C., Plenković-Moraj, A., Grgasović, T., 2008. Travertines and calcareous tufa deposits: an insight into diagenesis. *Geologia Croatica* 61 (2–3), 363–378.
- Guo, L., Riding, R., 1994. Origin and diagenesis of Quaternary travertine shrub fabrics, Rapalano Terme, central Italy. *Sedimentology* 41, 499–520.
- Jones, B., Kahle, C.F., 1995. Origin of endogenetic micrite in karst terrains: a case study from the Cayman Islands. *Journal of Sedimentary Research* A65, 283–293.
- Jones, B., Motyka, A., 1987. Biogenic structures and micrite in stalactites from Grand Cayman Island, British West Indies. *Canadian Journal of Earth Sciences* 24, 1402–1411.
- Jones, B., Renaut, R.W., 1995. Noncrystallographic dendrites from hot-spring deposits at Lake Bogoria, Kenya. *Journal of Sedimentary Research* A65, 154–169.
- Jones, B., Renaut, R.W., 2010. Calcareous spring deposits in continental settings. *Developments in Sedimentology* 61, 177–224.
- Koban, C.G., Schweigert, G., 1993. Microbial origin of travertine fabric: two examples from southern Germany (Pleistocene Stuttgart travertines and Miocene Riedöschingen travertine). *Facies* 29, 251–264.
- Konhauser, K., Riding, R., 2012. Bacterial biomineralization. In: Knoll, A.H., Canfield, D.E., Konhauser, K.O. (Eds.), *Fundamentals of Geobiology*. Blackwell Publishing Ltd., pp. 105–130.
- Korde, K.B., 1958. Sistematičeskoe položenie i stratigrafičeskoe značenie roda Epiphyton. *Byulleten' Moskovskogo Obshchestva Ispytateley Prirody, Otdel Geologičeskij* 33 (3), 156–157 (in Russian).
- Laval, B., Cady, S.L., Pollack, J.C., McKay, C.P., Bird, J.S., Grotzinger, J.P., Ford, D.C., Bohm, H., 2000. Modern freshwater microbialite analogues for ancient dendritic reef structures. *Nature* 407, 626–629.
- López-Martínez, R., Barragán, R., Beraldi-Campesi, H., Lánczos, T., Vidal-Romaní, J.R., Aubrecht, R., Bernal Uruchurtu, J.P., Puig, T.P., Espinasa-Pereña, R., 2016. Morphological and mineralogical characterization of speleothems from the Chimalacatepec lava tube system, Central Mexico. *International Journal of Speleology* 45, 11–122.
- Malinverno, A., Ryan, W.B., 1986. Extension in the Tyrrhenian Sea and shortening in the Apennines as result of arc migration driven by sinking of the lithosphere. *Tectonics* 5 (2), 227–245.
- Martín-García, R., Martín-Pérez, A., Alonso-Zarza, 2011. Weathering of host rock and corrosion over speleothems in Castañar cave, Spain: an example of a complex meteoric environment. *Carbonates and Evaporites* 26, 83–94.
- Mostardini, F., Merlini, S., 1986. Appennino centro-meridionale. Sezioni geologiche e proposta di modello strutturale. *Memorie della Società Geologica Italiana* 35, 177–202.
- Patacca, E., Scandone, P., 2007. Geology of Southern Apennines. *Bollettino della Società Geologica Italiana, Special Issue* 7, 75–119.
- Pentecost, A., 1990. The formation of continental carbonate shrubs: Mammoth Hot Springs, Wyoming. *Geological Magazine* 127, 159–168.
- Pentecost, A., 2005. *Travertine*. Springer-Verlag, Berlin.
- Pratt, B.R., 1984. Epiphyton and Renalcis – diagenetic microfossils from calcification of coccoid blue-green algae. *Journal of Sedimentary Petrology* 54 (3), 948–971.
- Riding, R., 1991a. Cambrian calcareous cyanobacteria and algae. In: Riding, R. (Ed.), *Calcareous Algae and Stromatolites*. Springer-Verlag, Berlin, pp. 305–334.
- Riding, R., 1991b. Calcified cyanobacteria. In: Riding, R. (Ed.), *Calcareous Algae and Stromatolites*. Springer-Verlag, Berlin, pp. 55–87.
- Riding, R., Voronova, L., 1982. Recent freshwater oscillatorian analogue of the Lower Palaeozoic calcareous alga *Angulocellularia*. *Lethaia* 15, 105–114.
- Riding, R., Voronova, L., 1985. Morphological groups and series in Cambrian calcareous algae. In: Toomey, D.F., Nitecki, M.H. (Eds.), *Paleoecology: Contemporary Research and Applications*. Springer-Verlag, Berlin, pp. 56–78.
- Săsăran, E., Bucur, I.I., Pleş, G., Riding, R., 2014. Late Jurassic *Epiphyton*-like cyanobacteria: indicators of long-term episodic variation in marine bioinduced microbial calcification? *Palaeogeography, Palaeoclimatology, Palaeoecology* 401, 122–131.
- Seard, C., Camoin, G., Rouchy, J.-M., Virgone, A., 2013. Composition, structure and evolution of a lacustrine carbonate margin dominated by microbialites: case study from the Green River formation (Eocene, Wyoming, USA). *Palaeogeography, Palaeoclimatology, Palaeoecology* 381–382, 128–144.
- Shiner, P., Beccacini, A., Mazzoli, S., 2004. Thin-skinned versus thick-skinned structural models for Apulian Carbonate Reservoirs: constraints from the Val D'Agri Fields. *Marine and Petroleum Geology* 21, 805–827.
- Vitale, S., Ciarcia, S., 2013. Tectono-stratigraphic and kinematic evolution of the southern Apennines/Calabria–Peloritani Terrane system (Italy). *Tectonophysics* 583, 164–182.
- Woo, J., Chough, S.K., Woo, A., 2008. Chambers of Epiphyton thalli in microbial buildups, Zhangxia formation (middle Cambrian), Shandong province, China. *Palaios* 23, 55–64.
- Zaninetti, L., 1978. Un organisme incertain de la Permien supérieur du Sud-Zagros, Iran. *Note du Laboratoire de Paléontologie de l'Université de Genève* 3, 17–19.